Free Entrainment Behavior in Sieve Trays

S. I. CHENG and A. J. TELLER

University of Florida, Gainesville, Florida

Analysis was made of the behavior of entrained particles in the zone between trays in a sieve tray column for the air-water system. The effects of drop-size distribution, projection velocity, drag, and gravity were evaluated with respect to the quantity of entrained liquid between trays. The drop-size distribution was found to be logarithmic in nature.

The entrainment as a function of distance above the froth is estimated in Equation (12) where d_H may be calculated from projection velocities and column superficial velocity for particle sizes greater than 400 μ.

Confirmation of the proposed entrainment equation via experimental data was achieved within an average deviation of 28%.

It was anticipated from the relationships developed that a leveling off of entrainment at zones in proximity to the froth and at escape velocity heights would be observed. Confirmation was evident at zones in proximity of the froth and upper zone tendencies were observed.

Investigation of the magnitude of entrainment in tray columns as a function of gross system conditions has been extensive. Most of this work has resulted in the development of empirical or quasiempirical relations which are applicable to specific types of internals and operating ranges. This report represents an effort to evaluate the entrainment phenomenon on the basis of the contributing behavior mechanisms.

The intensity of study in this field is reflected by the number of correlations of entrainment behavior. Souders and Brown (*17*) estimated the maximum column vapor velocity based on limiting entrainment, assuming all particles to be of equal size and following a Newton's law behavior. Eld (*4*) found that the estimate of the Souders and Brown relationship (*16*) was conservative and proposed a relationship assuming that the kinetic energy lost by the vapor is equal to the energy necessary to lift the liquid column prior to drop formation.

Simkin et al. (*16*) developed an empirical relationship, from data obtained in a bubble tray column, of entrainment with tray spacing, height of clear liquid above the slots, superficial vapor velocity, and the vapor and liquid densities.

Hunt et al. (9) established an empirical relationship for entrainment level in sieve trays as a function of height above the foam, superficial vapor velocity, and liquid surface tension and found that

$$e_w = 0.22\left(\frac{73}{\sigma}\right)\left(\frac{U}{S'}\right)^{3.2}$$

Atteridge et al. (*3*) studied bubble cap tower entrainment with respect to variations such as liquid-path length, cap spacing, number of slots, and liquid flow rate.

Holbrook and Baker (*8*) studied the effect of the column vapor velocity, plate spacing, amount of reflux, and surface tension on the bubble-plate entrainment.

Jones and Pyle (*10*) found that entrainment values from sieve trays were considerably less than those of bubble plates.

Pyott et al. (*12*) studied entrainment behavior with kerosene-air and water-air systems. The difficulty of comparison of entrainment effects of the two liquids in question was discussed.

Sherwood et al. (*15*) analyzed the effect of entrainment on column performance including treatment of both fractionation efficiency and the appearance of color in the distillate.

Strang's (*18*) work includes variation of the factors of column design, such as the distance between the plates, the height of the liquid on the plate, the size of slots in the bubble caps, and the insertion of a simple entrainment-separating device.

All the above correlations were developed from an empirical or quasi-theoretical standpoint, and although they may fit the conditions of the specific studies, they may not cover all types of tower designs and all vapor and liquid systems. The equation for entrainment prediction cannot be generalized if the actual mechanism of this phenomenon is not evaluated.

Davis (*4*) attempted to treat the entrainment problem theoretically. He explored the mechanism of drop formation from a single bubble and developed a relationship to predict the initial projection velocity of droplets from surface tension considerations. He also obtained a relationship relating the maximum height to which a drop can ascend, the diameter of the droplet, the velocity of the vapor in which the droplet is moving, and the initial projection velocity of the droplet.

Yusova (*19*) obtained the same result as Davis (*4*) in a similar study.

Newitt et al. (*12*) studied the formation of drops from bubbles obtained with a single orifice. Relationships were established to explain the entrainment phenomena, but extension to multiple perforations in actual columns was not made.

Garner et al. (*6*) studied the formation of drops in systems other than the air-water system and found that the mean droplet diameter changes with the mean bubble diameter as well as with the system.

Akselrod and Yosova (*2*) measured the liquid dispersion in the interplate

S. I. Cheng is with B. F. Goodrich Chemical Company, Cleveland, Ohio.

spacing and experimentally determined the relationship among the drop size, vapor velocity, and the maximum height a drop can ascend. Portions of their data are indicated in Figure 1 along with comparison with the approximate relation proposed.

Zenz et al. (*20*) assumed that the movement of fluidized particles in vapor is in streamline flow and developed an equation relating the particle diameter and the maximum height a solid particle can ascend, while Davis and Yosova assumed that the entrained droplet is in a vapor stream in turbulent motion.

In order to evaluate effectively the behavior of entrainment in the vapor zone in a tray column the various factors affecting the motion of entrained particles must be determined.

The quantity of entrainment at any level above the froth zone is a function of the height-drop size relationship and the size distribution relationship. The height-drop size relationship is a function of the effects of projection velocity, the vapor flow drag, and gravity. Via these factors the maximum height to which a particle can ascend may be determined.

The size distribution relationship of the particles projected from the froth zone is a function of the bubbling regime, the perforation velocities, liquid holdup, and the physical properties of the vapor and liquid streams.

Davis (*4*) evaluated the maximum height to which a particle could ascend in a vapor stream as a function of its projection velocity, the diameter of the particle, the velocity of the vapor stream, and the densities of the particle and the surrounding vapor. The relationship established by Davis is

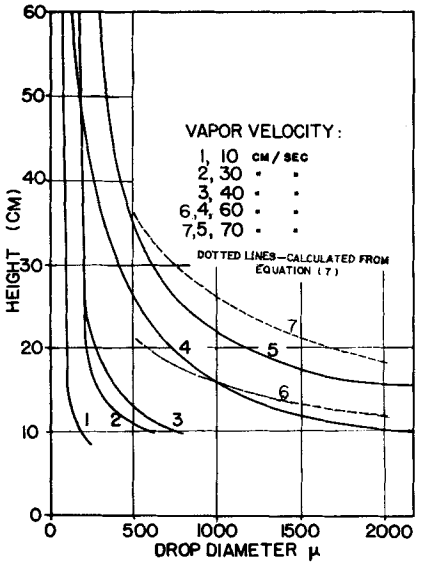

Fig. 1. Maximum ascent of drop as a function of drop diameter (2).

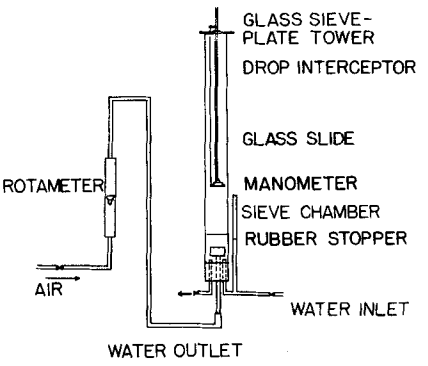

Fig. 2. Apparatus for free entrainment and drop-size distribution measurement.

$$H = \frac{q^2}{2g}\left\{\ln\left[1+\left(\frac{p-u}{q}\right)^2\right] - \ln\left[1-\left(\frac{u}{q}\right)^2\right]\right\} + \frac{uq}{2g}\left[2\tan^{-1}\left(\frac{p-u}{q}\right) + \ln\left(\frac{q+u}{q-u}\right)\right] \quad (1)$$

where

$$q^2 = \frac{4g}{3F}\left(\frac{\rho_L - \rho_G}{\rho_G}\right) do \quad (2)$$

Thus the diameter of a drop d_H that can reach a height H is a function of the variables indicated in Equation (3):

$$d_H = f\,(H, u, p, \rho_G, \rho_L) \quad (3)$$

However the function indicated in Equation (1) is not explicit, and direct determination of d_H cannot be made from values of the affecting variables. A solution can be obtained via calculation of drop diameters as a function of maximum height obtainable for the parameters of u and p. This approach can be utilized for evaluation of entrainment at various levels above the tray only if the projection velocities of particles are known as a function of the particle diameter and the physical properties of the system.

However for particles whose limiting or free-fall velocity is much greater than the vapor velocity and the projection velocity, a more explicit equation can be developed for determining the diameter of the particle ascending to a given maximum height.

Via expansion of Equation (1) in a series function there is obtained

$$H = \frac{q^2}{2g}\left[\frac{(p-u)^2}{q^2} - \frac{(p-u)^4}{2q^4} + \frac{(p-u)^6}{3q^6} - \frac{(p-u)^8}{4q^8} + \cdots\cdots\right] + \frac{u^2}{q^2} + \frac{u^4}{2q^4} + \frac{u^6}{3q^6} + \frac{u^8}{4q^8} + \cdots\cdots\Big] + \frac{uq}{g}\left[\frac{(p-u)}{q} - \frac{(p-u)^3}{3q^3} + \frac{(p-u)^5}{5q^5} - \frac{(p-u)^7}{7q^7} + \cdots\cdots\right] + \frac{uq}{2g}\left[\frac{u}{q} - \frac{u^3}{3q^3} + \frac{u^5}{5q^5} - \frac{u^7}{7q^7} + \cdots\cdots + \frac{u}{q} + \frac{u^3}{3q^3} + \frac{u^5}{3q^5} + \frac{u^7}{3q^7} + \cdots\cdots\Big] \quad (4)$$

Equation (4) may be solved via use of parameters of p and q for different particle sizes for various values of the superficial column velocity. However an approximate solution may be achieved if the minimum particle size considered is limited to 400 μ.

As indicated in Figure 9 the quantity of entrainment at a height of 5¼-in. above the foam, at a column velocity of 2 ft./sec. consists primarily of particles having diameters of 400 μ or greater (approximately 98%). Even at extremely low superficial velocities (1 ft./sec.) the particles having diameters less than 400 μ contribute less than 7% to the over-all entrainment at a level 3 in. above the foam.

With the condition of 400 μ as the minimum particle size considered the

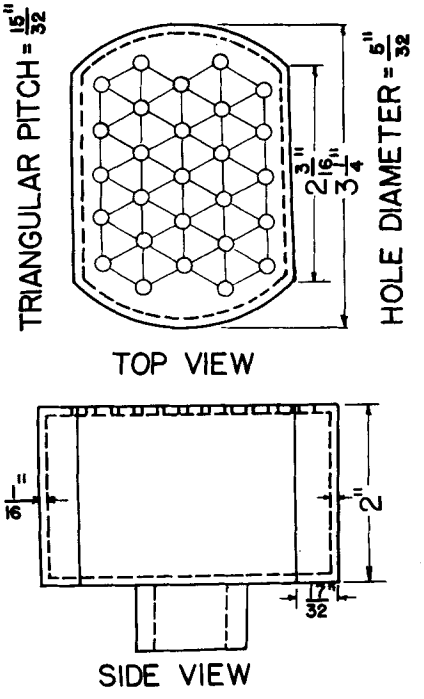

Fig. 3. Sieve chamber.

values of the quantities

$$\frac{p-u}{q} \text{ and } \frac{u}{q}$$

are generally less than 1 for the normal operating conditions of tray columns. Thus the terms beyond

$$\left(\frac{q}{p}\right)^2 = \frac{1/3\left[\left(\frac{u}{q}\right)^2 + 2\frac{p}{u}\right] - 1/4\left[2 + \left(\frac{p}{u}\right)^2\right]}{\frac{gH}{u^2} - \frac{1}{2}\left[2 + \left(\frac{p}{u}\right)^2\right]}$$

$$\frac{(p-u)^4}{2q^4} \text{ and } \frac{u^3}{3q^3}$$

in Equation (4) may be neglected, and there is still a reasonable degree of accuracy.

The limitation of this restriction to the general series function applies to the following column velocity conditions (water-air system).

Particle diameter, μ	Typical projection velocities, P—ft./sec. at $u = 1$ ft./sec.	$u = 2.3$ ft./sec.
400	4.3	9.1
500	3.6	7.6
700	3.4	7.2
1,000	3.3	7.0
2,000	2.4	6.0

The projection and terminal or escape velocities of water particles in air streams were obtained from data of Akselrod et al. (2), Aiba and Yamada (22), Perry's Handbook (21).

Thus within the minimum particle size limitation Equation (4) may be approximated by the expression

$$H = \frac{1}{2g}(p^2 + 2u^2) + \frac{1}{12gq^2}$$
$$[3u^4 - 3(p-u)^4 - 4u(p-u)^3] \quad (5)$$

The terminal or escape velocity is made the dependent variable by transformation of Equation (5):

$$q^2 = \frac{4u^4 - 6u^2p^2 + 8up^3 - 3p^4}{12gH - 6(p^2 + u^2)} \quad (6)$$

If Equation (6) is rewritten in the form of

it is noted that the value of the numerator is zero when $p/u = 16/9$, and $H = 2.58\ u^2/g$. For the range of particle sizes for which this analysis applies, the linear velocities at the condition of $p/u = 16/9$ exceed 10 ft./sec. for particle sizes less than 1,000 μ. For the particle size 2,000 μ the superficial column velocity for the condition $p/u = 16/9$ is in the range of 2.5 ft./sec. resulting in a maximum height of ascent of this particle size of 5.5 in. above the froth.

q ft./sec.	Superficial column vapor velocity, (ft./sec.) Minimum	Maximum based on extrapolated values
5.2	0	2 (2)
7.0	0	4
9.7	0	9.7
13	0	13
22	0	22

The value of p/u for particle sizes less than 1,000 μ will exceed 16/9 for all commercial ranges of operation.

The particle size may be predicted from its maximum height of ascent by substituting for q^2, its equivalent, in Equation (2). Thus

$$d_H = \frac{3F}{4g}\frac{\rho_G}{\rho_L - \rho_G}\left[\frac{4u^4 - 6p^2u^2 + 8pu^3 - 3p^4}{12gH - 6(p^2 + 2u^2)}\right] \quad (7)$$

which is applicable only to particle sizes greater than 400 μ for the linear velocities stipulated.

A comparison of the results obtained from application of Equation (7), and data obtained by Akselrod and Yosova (2) is indicated in Figure 1.

It is noted from Equation (7) that the particle size of the entrained liquid will decrease with increase in distance from the tray, which is confirmed by the observation of Akselrod and Yosova (2).

In order to establish a relationship for the determination of the quantity of entrainment, with the particle size height of ascent relationship, the distribution of sizes of particles projected from the froth surface must be known.

Since the weight of a particle of a given diameter x is equal to $\pi/6\rho L\ x^3$, the weight of entrained particles up to a diameter d_H may be expressed as

$$W_H = \frac{\pi}{6}\cdot\rho_L\frac{N_D}{\sigma\sqrt{2\pi}}\int_{x=0}^{x=d_H} f(x)\,dx \quad (9)$$

where $f(x)$ is the distribution function for particles in the zone between trays.

The diameter of the largest particle d_H reaching the height H above the foam for which the weight of entrainment is to be determined via use of Equation (9) may be obtained from Equation (7) or Figure 1. Solution must be made by solving for the value H as a function of the particle diameter d_H, since the particle diameter, the projection velocity, and the superficial column velocity are dependent variables.

The only distribution data available for entrained particles were those obtained by Newitt (12) from bursting of bubbles emanating from a single perforation. The distribution was found to be normal. If such were the case in tray columns where multiple perforations exist, the weight of entrained particles could be represented by the relationship

$$W_H = \frac{\pi\,\rho_L}{6}\frac{N_D}{\sigma\sqrt{2\pi}}\int_{x=0}^{x=d_H} x^3 \exp\left[-\frac{1}{2}\left(\frac{x-\bar{x}}{\sigma}\right)^2\right] dx \quad (10)$$

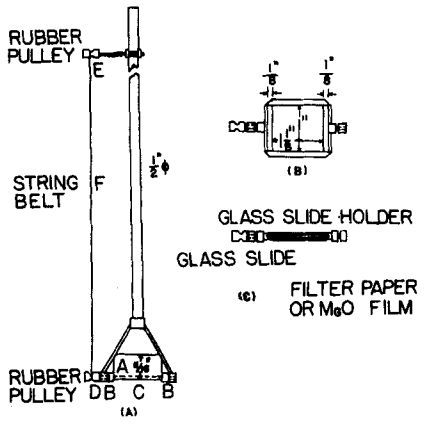

Fig. 4. Drop interceptor.

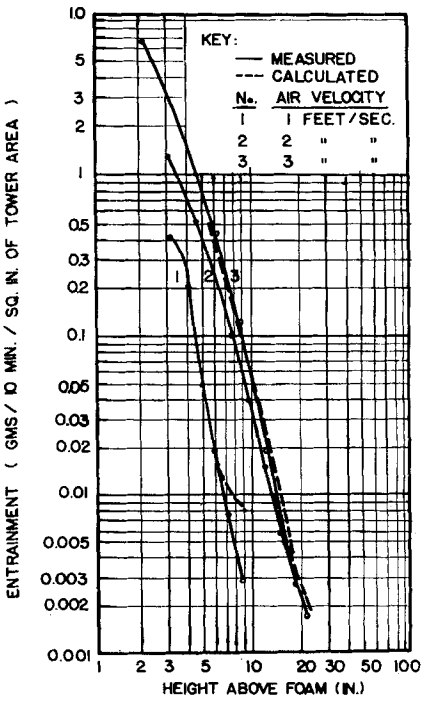

Fig. 5. Comparison between measured and calculated entrainment.

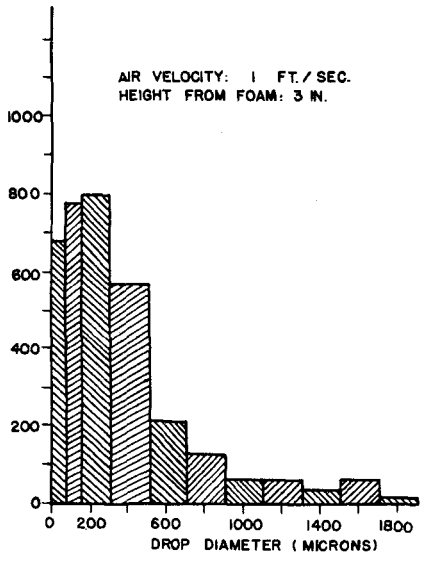

Fig. 6. Histogram of entrained drops from sieve plate.

Table 1. Example of Numerical Integration of Weight of Drops in Logarithmic Distribution

Air velocity, 2 ft./sec.
Height above surface, 5¼ in.

Average particle diameter, μ	Accumulative, %
50	0.0026
100	0.0692
200	0.8362
400	1.3702
600	9.8202
800	20.82
1,000	33.79
1,200	47.45
1,400	61.15
1,600	74.8
1,800	87.9
2,000	100

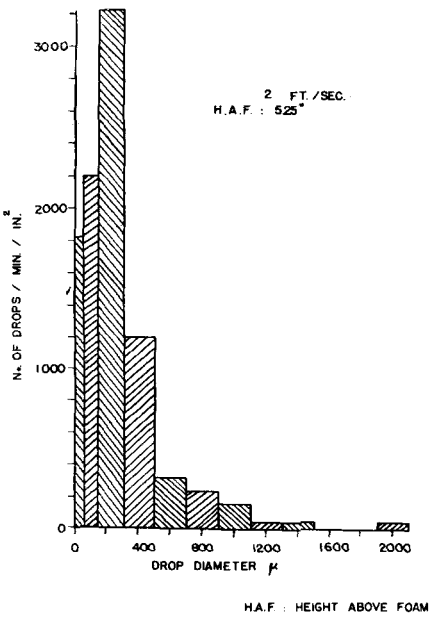

Fig. 7. Histogram of entrained drops from sieve plate.

It was necessary however to ascertain the actual distribution obtained from multiple perforations and the quantities of entrained liquid in order to test the relationships established.

APPARATUS AND PROCEDURE

The study was concerned with the air-water system with a sieve plate having 5/32-in. diameter perforations on 15/32-in. triangular pitch and was established primarily to evaluate the applicability of the hypothesis presented.

The evaluation unit (Figure 2) consisted of a shell (3¾-in. I.D.) containing a perforated tray 8% open (Figure 3) with perforations covering 70% of the tray cross section. A cylindrical section equivalent to the tray cross section extended 2 in. below the tray to promote effective distribution of the air prior to entering the perforations. The equivalent stagnant clear liquid level on the tray was measured with a manometer. Air was metered in through a rotameter. The drop interceptor for measurement of both the quantity of entrainment and the size distribution of the entrained liquid droplets is indicated in Figure 4. The interceptor consisted of a holder box suspended by a ½-in. diameter rod. The interceptor box contained a 1 sq. in. rotating glass slide which could be covered with a magnesium oxide film or to which could be attached a filter paper absorber. The measurement surface was exposed to the entrainment at preestablished heights above the froth via rotation of the glass slide into the interception position. After a given time for interception the slide was rotated back to its initial position with the exposed surface facing upward.

For size-distribution studies the exposed glass slide coated with magnesium oxide (created by burning magnesium ribbon under the glass) was placed in the film section of a slide projector. The counts and sizes were then determined at a magnification factor of 29. Evaluation of the work of Akselrod (*1*) indicated that nearly all drops ascend to a height within 3 in. of the froth and that (via extrapolation and direct measurements) the deviation of size distribution at this height from the initial projection frequency function is small. This measured or extrapolated distribution may then be taken as the initial projection frequency function.

The weight of the entrained liquid per unit time was measured by the weight of captured liquid on the filter paper attached to the glass slide for given exposure times. Prior and subsequent to the measurement procedure the filter paper was kept in a vessel exposed to air saturated with water vapor at 20° to 25°C. Interception periods, providing reproducibility, varied from 15 sec. at levels in proximity to the plate to 10 min. at high levels above the froth.

During all runs the equivalent clear stagnant liquid was maintained at a contant value of 1½ in. Runs were made at air rates from 1 ft./sec. to 4 ft./sec. Entrainment values and distributions were obtained at heights of 2 to 30 in. above the froth surface. Wave action was noted in the tray similar to that observed in larger columns. The heights above the foam reported are based on the actual foam height measured.

PARTICLE-SIZE DISTRIBUTION

The size distribution of the entrained particles for superficial column velocities at various levels above the froth are represented in Figures 6, 7, and 8. Data for superficial velocities of 1, 2, and 3 ft./sec. at levels of 3 to 26-in. above the froth are available.* Since drops having diameters in the range of 2,000 μ do not rise to significant levels above the foam, the deviation of drop size from the initial projection distribution function increases with increase in height above the foam.

Measurements in proximity to the foam were not feasible owing to the very high level of entrainment and side splashing of the liquid. Thus the frequency function was evaluated from data at the lowest level, where accurate measurements were possible.

CALIBRATION OF DROP SIZE MEASUREMENT

The size of drop image on a magnesium oxide film may be different from the actual drop size owing to impaction and spreading. Thus comparison was made between the measured entrainment and the value obtained from summation of weights of drops measured by magnesium oxide film. The results are shown in Figure 5 for air rate equal to 1, 2, 3 ft./sec., respectively.

Since the values are almost coincident, the diameters of drop images on magnesium oxide film may be taken as the actual diameters of drops in the evaluation of size distribution. The small deviation of the entrainment by absorption and by summation from distribution data obtained at higher levels above the foam may be due to the fact that the efficiency of absorption of water droplets from air currents by filter papers becomes smaller when the size droplets is very small.

As indicated by the histograms of the size of the entrained particles (Figures 6 and 7) they are obviously not in normal distribution as indicated by Newitt (*12*) for single perforation sources. A logarithmic normal distribution was fitted in accordance with the following method.

* Tabular material has been deposited as document 6620 with tht American Documentation Institute, Photoduplication Service, Library of Congress, Washington 25, D. C., and may be obtained for $1.25 for photoprints or for 35-mm. microfilm.

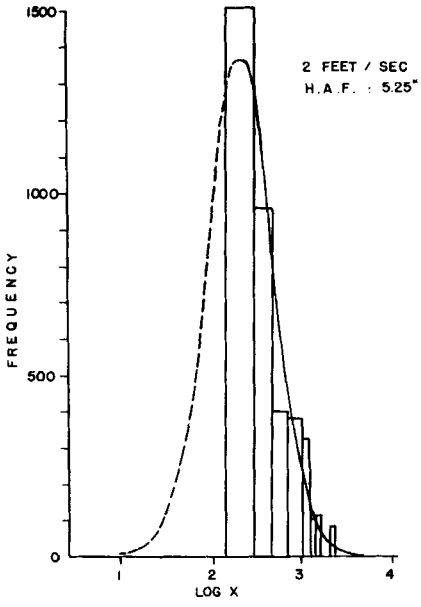

Fig. 8. Fitting of histogram to log normal curve.

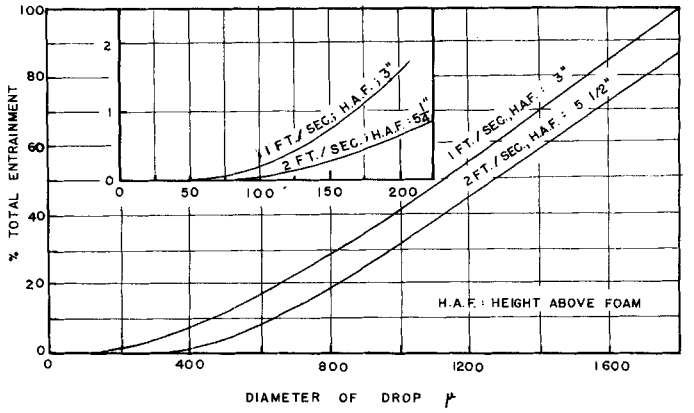

Fig. 9. Accumulation of weights of entrained drops in log normal curve.

It was difficult to measure the population of particles having diameters of less than 50 μ, and this population was created most probably by the result of explosion of thin liquid domes. Thus only the upper levels of particle sizes were used in the determination of the distribution function (greater than 50 μ size) (Figure 8). This procedure appeared reasonable, since the major contribution to entrainment weight is made by these larger-size particles. The method is similar to that used by Newitt et al. (*12*).

The method indicated by Hoel (7) was used to calculate the theoretical frequency of various drop sizes, and these frequencies were compared with observed frequencies. A typical distribution confirmation is indicated in Figure 8. From this comparison it appears reasonable that the entrainment from a sieve plate for the air-water system is nearly in logarithmic distribution. This is a behavior similar to that observed for formation of bubbles in a liquid by Liebson et al. (*11*).

The form of the frequency function is

$$f(x) = \frac{1}{\sigma\sqrt{2\pi}} \exp\left[-\frac{1}{2}\left(\frac{\log x - \log \bar{x}}{\sigma}\right)^2\right] \quad (11)$$

and the total entrainment at height H is indicated by substitution of this function in Equation (9):

$$W_T = \frac{\pi}{6}\frac{N_D \rho_L}{\sigma\sqrt{2\pi}} \int_{x=0}^{x=d_H} x^3 \exp\left[-\frac{1}{2}\left(\frac{\log x - \log \bar{x}}{\sigma}\right)^2\right] d \log x \quad (12)$$

This relationship is difficult to solve analytically but may be solved graphically or by numerical summation. An example of solution by numerical summation is indicated in Figure 9 and Table 1.

CALCULATION OF ENTRAINMENT

By logarithmic distribution the mean diameter of drops at 1 ft./sec. and 2 ft./sec. was found to be 200 μ. The standard deviations in these cases were found to be 0.436 and 0.349 respectively. The integrated weights of entrainment per unit time as a function of particle diameter were calculated by application of Equations (11) and (12) for the conditions of $u_s = 1$ ft./sec. and height above foam of 3 in., and for conditions $U_s = 2$ ft./sec. and height above foam of 5¼ in. These relationships are indicated in Figure 9.

The free entrainment for the air-water system was found to be a function of the superficial velocity and the height above the foam, similar in shape (Figures 10, 10*a*, and 11 and Tables 1A-1D)* to that indicated by (*1*) for captured entrainment. However in contradiction to the predicted behavior by Hunt et al. (9) for captured entrainment, separate curves were obtained for different superficial velocities with significant differences observable at 4 ft./sec. This behavior reflects the influence of perforation velocities on the size distribution of the entrained particles.

The shape of the curves may be anticipated by application of Equation (1) or Figure 1 and Equation (12) or approximately by Equations (7) and (12). Although the change in maximum particle diameter in proximity to the froth is extremely sensitive to change in height above the froth due to the rapid change of the value of the denominator in Equation (7), $12gH$-$6(p^2 + 2u^2)$, the quantity of these particles in the range of 2,500 μ or greater is so small that the quantity of entrainment is not affected by their disappearance. Thus a relatively constant maximum entrainment may be observed at levels in proximity to the froth. However entrainment level at this zone may be affected by jetting and splashing due to wave action of the liquid, thus resulting in an unpredictable actual level of entrainment.

There is a tendency for an approach to a constant level of entrainment beyond a critical height above the foam as a function of the column velocity. This asymptotic behavior may be anticipated in general from Equation (7), since with decrease in particle size with height above the foam the value of p becomes large with respect to u and q. Thus d_H becomes less sensitive in relation to H.

However, a more exact analysis may be made with Equation (1). With in-

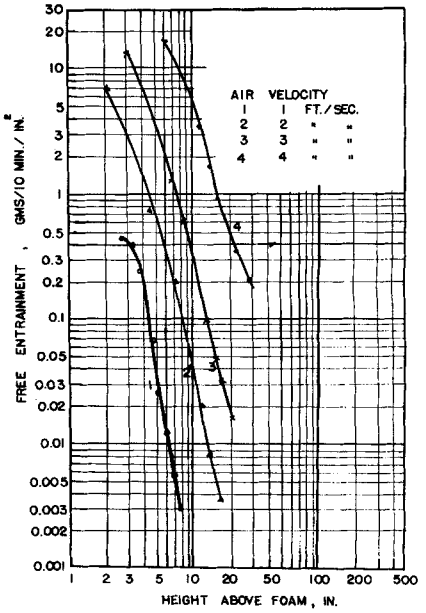

Fig. 10. Relationship between free entrainment and height above foam.

* See footnote on page 285.

crease in height the surviving particles (sizes less than 400 μ) have terminal velocities similar to those of the superficial velocities. Thus the term $\ln\left(\frac{q+u}{q-u}\right)$ in Equation (1) approaches infinity for particle sizes whose terminal velocities approach the linear velocities. The concentration of these particles will be insensitive to height above the tray.

This nonlinear logarithmic behavior at least in regions in proximity to the froth has been confirmed by FRI tests (*1*) and is indicated in the curvatures of the lines in Figure 10.

On the basis of the cumulative entrainment of Figure 9 based on the particle size distribution functions and the maximum particle size reaching a given height above the foam obtained from either Equation (7) or Figure 1, the entrainment level at various levels in the column were calculated for superficial column velocities of 1 ft./sec. and 2 ft./sec. If the maximum height of attainment for particle sizes less than 400 μ is required, then the original Davis' Equation (1) must be used.

The comparison with observed values are indicated in Figure 11. The results are promising in view of the experimental errors involved in measurements. The average deviation for the superficial velocity of 1 ft./sec. was 28% and 25% for the superficial velocity of 2 ft./sec.

Large deviations were observed from predicted values primarily at elevated heights above the foam where the measured quantity of entrainment was in the range of 0.0002 g./min./sq. in. of tower. The value is of such a small magnitude that errors in the range of accuracy of the balance can produce a considerable percentage error. Thus it appears that with the degree of corroboration achieved that the magnitude free entrainment can be predicted from functions of the drop-size distribution and a height-diameter relationship.

This study represents an initial investigation with respect to entrainment behavior in the air-water system. The next step in an understanding of this phenomenon; the relationship of free entrainment and the actual quantity of liquid captured by the tray above has not yet been established. The relationship of the entrainment actually passing through the perforations and the free entrainment is not a simple relationship of area proportion, inasmuch as eddy formation in the vapor below the tray and reentrainment contribute to the phenomenon.

However the behavior of free entrainment indicates that there exists

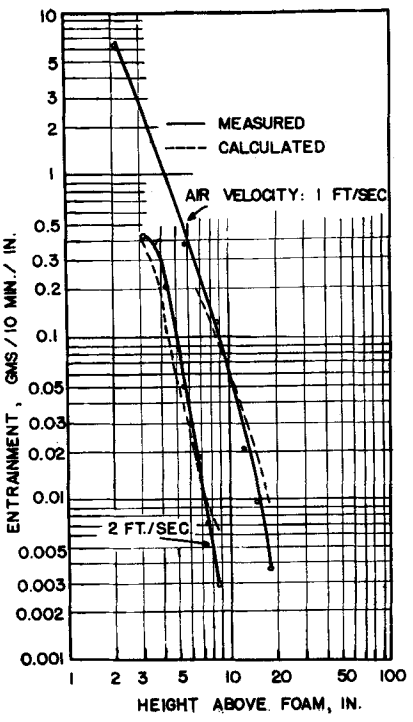

Fig. 11. Comparison between measured and calculated entrainment.

tray spacings beyond which an increase will not cause the significant dimunition of the quantity of entrained liquid.

NOTATION

D_B = diameter of vapor bubble
d_H = diameter of drop that can ascend to height H
d_M = maximum drop diameter
d_o = diameter of drop
e_w = weight of entrainment
F = friction constant
H = height above liquid surface
N_D = number of drops
p = projection velocity of drops or velocity at which the drop is ejected from the liquid surface
P_o = absolute vapor pressure
P = pressure difference
q = limiting or terminal velocity of drop
Q_G = volumetric gas flow rate per perforation
r = depth of submergence of base of bubble
R = radius of vapor bubble
R' = resistance of vapor to movement of drop
S' = effective plate distance, top of foam to tray above
t = time of application of impulse force to jet
u = vapor velocity (superficial)
V_B = volume of vapor bubble
W_H = free entrainment at height H
W_T = total entrainment at liquid surface
x = diameter of drop as variable in frequency function
x_o = most probable drop diameter
$\overline{X}$ = mean diameter of drops
$f(x)$ = frequency function of drop sizes

Greek Letters

σ = standard deviation of drop diameters
ρ_w = density of water
ρ_G = density of vapor
ρ_L = density of liquid
μ = viscosity of liquid

LITERATURE CITED

1. A.I.Ch.E. Research Committee, "Bubble Cap Manual," Am. Inst. Chem. Engrs., New York (1958).
2. Akselrod, L. S., and G. M. Yosova, *J. Appl. Chem.* (*USSR*), **30**, 739 (1957).
3. Heridge, P. T., E. J. Lemieux, W. C. Schreiner, and R. A. Sundback, *A.I.Ch.E. Journal*, **2**, 3 (1956).
4. Davis, R. F., *Proc. Inst. Mech. Engrs.*, **144**, 216 (1940).
5. Eld, A. C., *Petrol. Refiner*, **32**, (5), 157 (1953).
6. Garner, F. H., and S. R. M. Lacey, *Trans. Inst. Chem. Engrs.*, **32**, 222 (1954).
7. Hoel, P. G., "Introduction to Mathematical Statistics," pp. 76-82, Chapman and Hall (1958).
8. Holbrook, G. E., and E. M. Baker, *Trans. Amer. Inst. Chem. Engrs.*, **30**, 50 (1934).
9. Hunt, C. A., P. M. Hanson, and C. R. Wilke, *A.I.Ch.E. Journal*, **1**, 441 (1955).
10. Jones, J. B., and C. Pyle, *Chem. Eng. Progr.*, **51**, 424 (1955).
11. Liebson, I., E. G. Holcomb, A. G. Cucoso, J. J. Jacmie, *A.I.Ch.E. Journal*, **2**, 296 (1956).
12. Newitt, D. M., N. Dombrowski, and F. H. Knelman, *Trans. Inst. Chem. Engrs.*, **32**, 244 (1954).
13. Pyott, W. I., C. A. Jackson, and R. L. Huntington, *Ind. Eng. Chem.*, **27**, 821 (1935).
14. Quigley, C. J., A. J. Johnson, and B. L. Harris, *Chem. Eng. Progr. Symposium Ser. No. 16*, **51** (1955).
15. Sherwood, T. K., and F. J. Jenny, *Ind. Eng. Chem.*, **27**, 265 (1935).
16. Simkin, D. J., C. P. Strand, and R. B. Olney, *Chem. Eng. Progr.*, **50**, 565 (1954).
17. Sounders, M., and G. G. Brown, *Ind. Eng. Chem.*, **26**, 98 (1935).
18. Strang, L. C., *Trans. Inst. Chem. Engrs.*, **12**, 169 (1934).
19. Yosova, G. M., Candidates dissertation, Sci. Res. Inst., USSR (1954).
20. Zenz, F. A., and N. A. Weil, *A.I.Ch.E. Journal*, **4**, 472 (1958).
21. Perry, J. H., "Chemical Engineers Handbook," p. 1021, McGraw-Hill, New York.
22. Aiba, Shuichi, and Toyokara Yamada, *A.I.Ch.E. Journal*, **5**, No. 4, 506 (1959).

Manuscript received February 10, 1960; revision received October 6, 1960; paper accepted October 10, 1960. Paper presented at A.I.Ch.E. Mexico City meeting.